

# STUDY OF ACOUSTIC EMISSION DATA ANALYSIS TOOLS FOR STRUCTURAL HEALTH MONITORING APPLICATIONS

MANINDRA R. KAPHLE, ANDY C.C. TAN, DAVID P. THAMBIRATNAM  
and TOMMY H.T. CHAN

Queensland University of Technology, 2 George St, Brisbane, Australia

## Abstract

Though acoustic emission (AE) is becoming a popular non-destructive testing (NDT) technique for structural health monitoring (SHM) of civil, mechanical and aerospace structures, challenge of effective analysis of recorded data still exists. This paper explores various tools for analysis of recorded AE data to address two primary challenges: discriminating signals from different sources and quantifying damage levels for severity assessment. It is believed such analysis will help in better understanding of mechanisms of AE generation and help enhance the monitoring capability of AE technique.

## 1. Introduction

Acoustic emission (AE) technique is one of the several diagnostic techniques used for structural health monitoring (SHM) applications. AE technique involves recording the stress waves by means of sensors and appropriate data acquisition system and subsequent analysis of the recorded signals to gather information about the nature of the source of emission [1]. AE technique is highly sensitive to crack activity (active cracks generate while dormant ones do not) and can provide continuous in-situ monitoring. Despite the advantages, successful use of AE technique for structural health monitoring applications has several challenges. A number of spurious sources can also produce AE signals, which can mask genuine damage related signals; hence, it is important to accurately sort extraneous noise from crack based AE [2]. Another important challenge is quantifying the level of damage to assess severity of sources.

Recording and analysis of the complete AE signal waveforms is now common. Though the signals captured by sensors are affected by the medium of propagation and the sensor characteristics, the signals still contain some information about the nature of the source [3]. Hence, complete waveform based analysis approach is believed to yield better results than traditional approach of using parameters alone in source discrimination. To analyse the recorded waveforms, frequency analysis using Fourier transform and time-frequency analysis using short-time Fourier transform (STFT) and wavelet analysis are popular tools. Ratios of energy distribution in different frequency bands from wavelet analysis has been used to identify different potential failure modes in composites [4]. Further, as similar source mechanisms emit similar signals, search for similarity also helps in source discrimination. Cross-correlation coefficients in time domain and magnitude squared coherence (MSC) in frequency domain can be used to check if signals are similar or not [3, 5, 6]. Quantifying damage level is usually attempted using different AE signal parameters or a combination of these. A traditional approach is the b-value analysis, see [7, 8]. It has been found to change during different stages of damage, for example when microcracks occur in the early stages of damage, the b-value is high but becomes low when macrocracks begin to occur [8], making the b-value a candidate to judge damage progress [9]. The b-value has been recently modified by using statistical values of amplitude distribution (mean and standard deviation) and the newer method is referred as improved b-value (Ib-value) [10]. Ib value improves calculation by selecting the amplitude limits of the linear range of the cumulative

frequency distribution data of AE [11]. Ib-value is usually calculated for a certain number of events (generally ranging from 50 to 100) during the test.

This paper aims to explore different data analysis approaches for source discrimination and severity assessment, by analysing AE data recorded from testing in laboratory.

## 2. EXPERIMENTATION

### 2.1 Source differentiation

For source differentiation experiments, two sources of AE signals were generated by (a) breaking 0.5-mm pencil leads (Hsu-Nielsen source) and (b) dropping steel balls (6-mm diameter) from a height of 15 cm on a 4 m long steel beam. Ten sets of each test were carried out. A four-channel  $\mu$ -disp PAC (Physical Acoustics Corporation) system along with two R15 $\alpha$  sensors (made by PAC, resonant at 150 kHz) placed at distances of 1.5 m (Sensor S1) and 3 m (Sensor S2) from the source were used for data acquisition. The sensors were coupled using vacuum grease and magnetic holders. Preamplifiers were used with gain set at 40 dB. The signals were bandpass filtered between 20-400 kHz, as most signals were expected in this range. For each hit, data was acquired at a sampling rate of 1 MHz and recorded for 15-ms duration.

Recorded signals were analysed, first by calculating energy distributions in different frequency bands from STFT analysis. Next, cross-correlation coefficient and magnitude-squared coherence were calculated using Matlab commands ‘xcorr’ and ‘mscohore’ to check signal similarity in time and frequency domains, respectively. The command ‘xcorr’ gives the value of 1 for two identical signals. Similarly, ‘mscohore’ gives values lying between 0 and 1, which indicate how well two signals correspond to each other at each frequency; with the value of 1 indicating exact match [12].

### 2.2 Severity assessment

For damage quantification experiment, three-point bending tests were carried on steel pieces (300-mm long, 25-mm wide and 10-mm thick, with a small 45° V-notch in the middle to initiate the crack growth). Instron tensile machine with 100 kN load-cell was used to apply loads to three specimens at loading rates of 1, 2 and 3 mm/min each. To set the threshold value for recording and ensure sensors were performing correctly, pencil-lead breaks (0.5-mm diameter HB leads) were carried out near the crack tip. The value of 60 dB was used as the threshold value in each case, as this value was found to prevent the recording of lower amplitude reflected signals from the pencil-lead break tests. Same system and settings were used for AE data acquisition. Two R15 $\alpha$  resonant sensors were placed at the ends of the specimens equidistant from the crack in order to record signals.

## 3. Results and Discussion

### 3.1 Source differentiation

Typical pencil-lead break (PLB) and ball-drop (BD) signals recorded by sensor S1 along with their time-frequency STFT representation calculated using Time-frequency toolbox [13] are shown in Figs. 1 and 2, respectively. Only initial 2 ms of data were used for analysis purposes. The BD signal shows higher energy levels but at lower frequency bands compared to the PLB signal. To study energy distribution with frequency, energies across the total time were summed and the values normalized with respect to total energy across all times and frequencies. Values of these energy ratios against frequencies for ten PLBs and ten BDs are shown in Fig. 3.

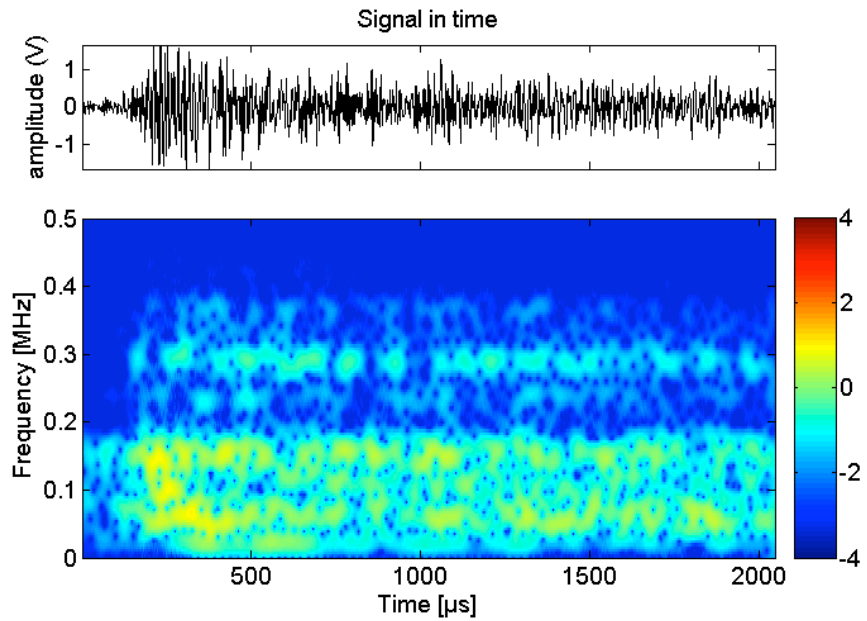


Fig. 1. PLB signal (upper) along with its STFT representation (below).

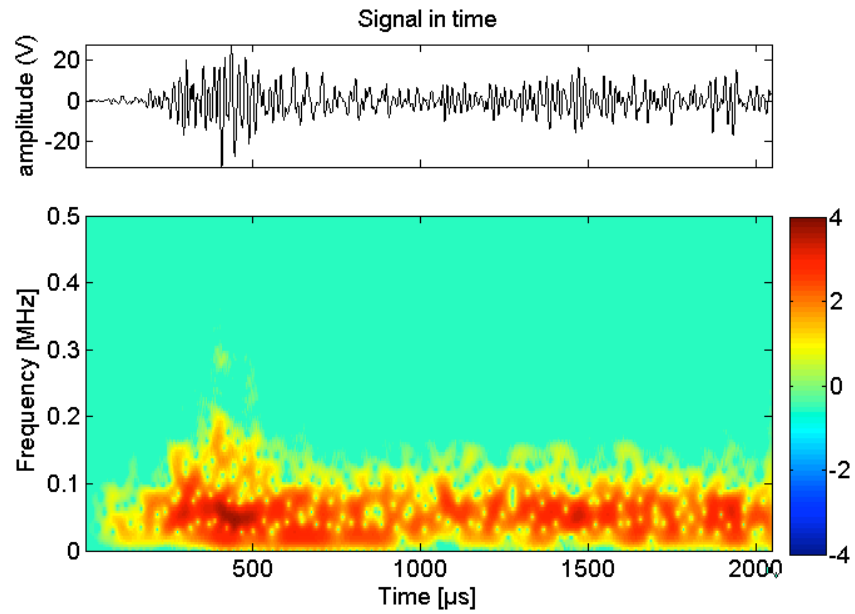


Fig. 2. BD signal (upper) along with its STFT representation (below).

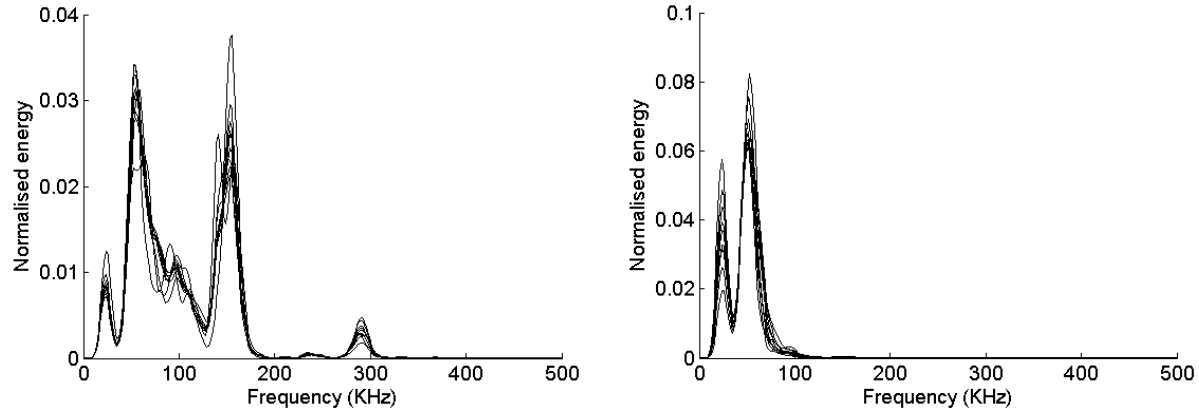


Fig. 3 Distribution of energy against frequencies for PLB and BD signals.

For PLB signals, most energy lies around two peak frequencies of 70 kHz and 170 kHz and small peak at 300 kHz. For BD signals energy is distributed around 70 kHz only. This distinct distribution of energy can differentiate sources.

*Cross-correlation analysis:* Using the PLB signal (Fig. 1) as the template signal, cross-correlation was performed with the remaining nine PLB signals recorded by S1 and with the ten BD signals, also recorded by S1. A sample result is shown in Fig. 4.

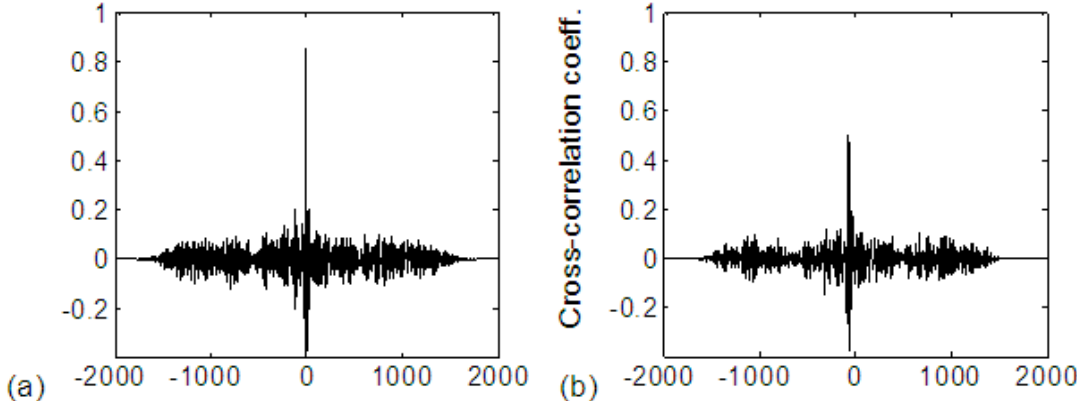


Fig. 4(a) Cross-correlation between two PLB signals (b) Cross-correlation between PLB and BD signals

High cross-correlation (maximum value 0.86) is seen for two PLB signals in Fig. 4a while in Fig. 4b the maximum value is only about 0.5. Cross-correlation of the template PLB signal with remaining nine PLB tests gave an average maximum value of 0.87 (actual: 0.80-0.91) while that for PLB-BD correlation was 0.48 (actual: 0.38-0.54). This difference in maximum cross-correlation values can be used as a criterion for signal discrimination.

*Magnitude squared coherence analysis:* Magnitude-squared coherence (MSC) analysis was performed using the same template PLB (Fig. 1) and rest of the signals recorded by the sensor S1. A typical plot of MSC values versus frequencies with a PLB signal is shown in Fig. 5a and that with a BD signal is shown in Fig. 5b. Figure 5a indicates closer match of frequencies between the PLB signals in the range 20 - 400 kHz (bandpass range), with an average value of 0.73. On the other hand, Fig. 5b indicates less coherence in that range, with an average MSC value of 0.27.

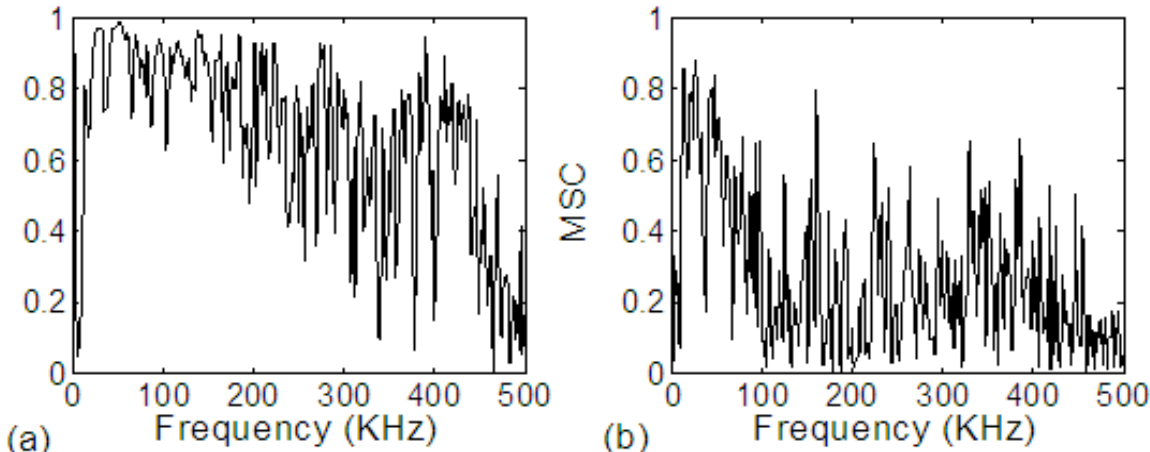


Fig. 5. MSC values versus frequencies. (a) two PLB signals, (b) PLB and BD signals.

While calculating MSC values of the template PLB with the other PLB signals, mean values lie in the range 0.71–0.75, while mean MSC values of the PLB signal with other ten BD signals lie in the much smaller range of 0.25–0.35 with a mean value of 0.29. Again, this distinct difference shows the usefulness of MSC values in signal discrimination.

It is noted that while performing cross-correlation and MSC between the template PLB-S1 signal (Fig. 1) and ten PLBs of sensor S2, very low values were obtained (less than the values obtained in earlier analysis between the PLB and BD signals recorded by the same sensor S1). Nevertheless, cross-correlation and MSC could identify same sources from same distance and this has significant advantage in SHM applications. For example, while monitoring the activity of a crack (finding it is active or benign) in gusset plate of a bridge in real time, being able to automatically filter out AE signals due to traffic using a template signal will significantly reduce the data load.

### 3.2 Severity assessment

The variation of load with time (to 500 s) for a three-point bending test along with the amplitudes of the hits for one sensor is shown in Fig. 6. When yielding starts, a large number of AE signals with higher amplitudes and energies were recorded in the region of transition between the elastic and plastic deformation. The first visual signs of crack occurred after most of the AE hits, generally when the load reached the peak value. After this, the load decreased and the crack continued to grow but few new AE hits occurred. It is noted that these findings have been well known and have been reported previously.

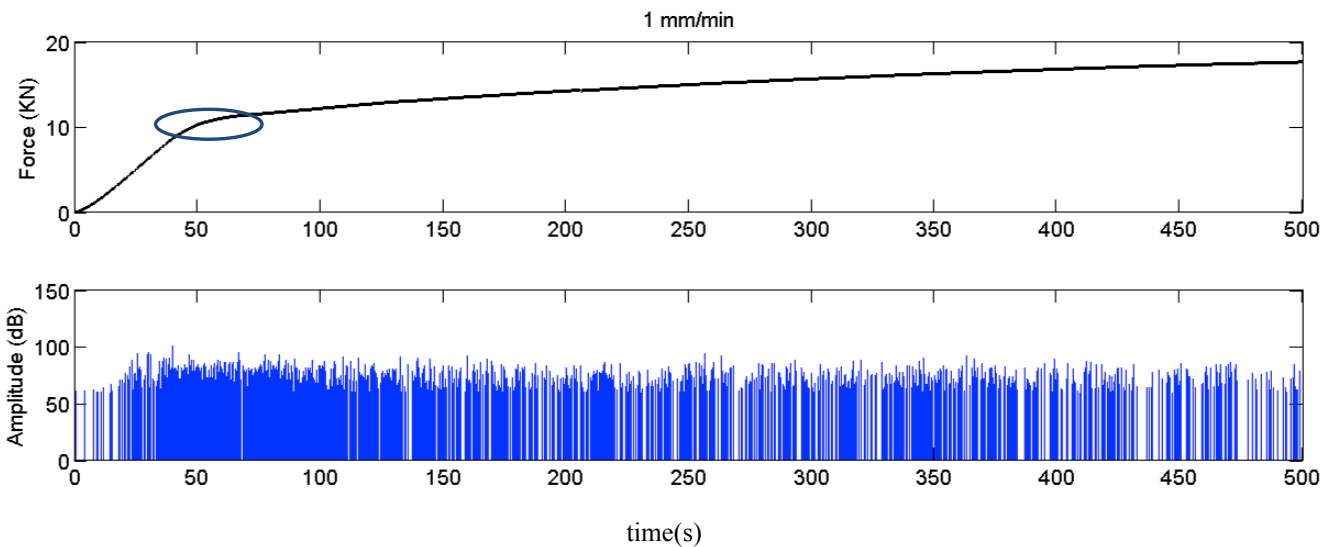


Fig. 6. Variation of force and AE amplitude with time for 1 mm/min loading.

*b and Ib value analysis:* The cumulative amplitude distribution (number of events vs. amplitude), showed that the linearity exists only in the earlier to middle portion of the distribution. For example, the distribution of amplitudes for 1 mm/min loading case is shown in Fig. 7.

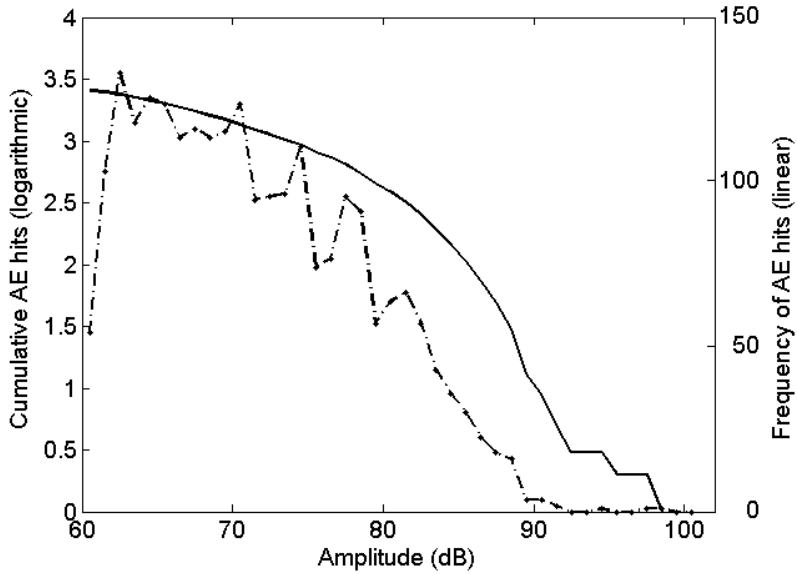


Fig. 7. Frequency (linear, dashed line) and cumulative frequency (logarithmic, solid line) of AE hits against amplitude.

Ib-value was utilized to calculate the slope in this linear region [10] using sets of 100 events with a lag of 20 events as done in [14], that is, the Ib value is first calculated for the group of the events 1-100, then 21-120, followed by 41-140 and so on. A sample Ib value calculation for first set of 1 mm/loading case is shown in Fig. 8. The results showing the variation in Ib-value (multiplied by 20 as suggested) with time for the three loading cases are shown in Fig. 9.

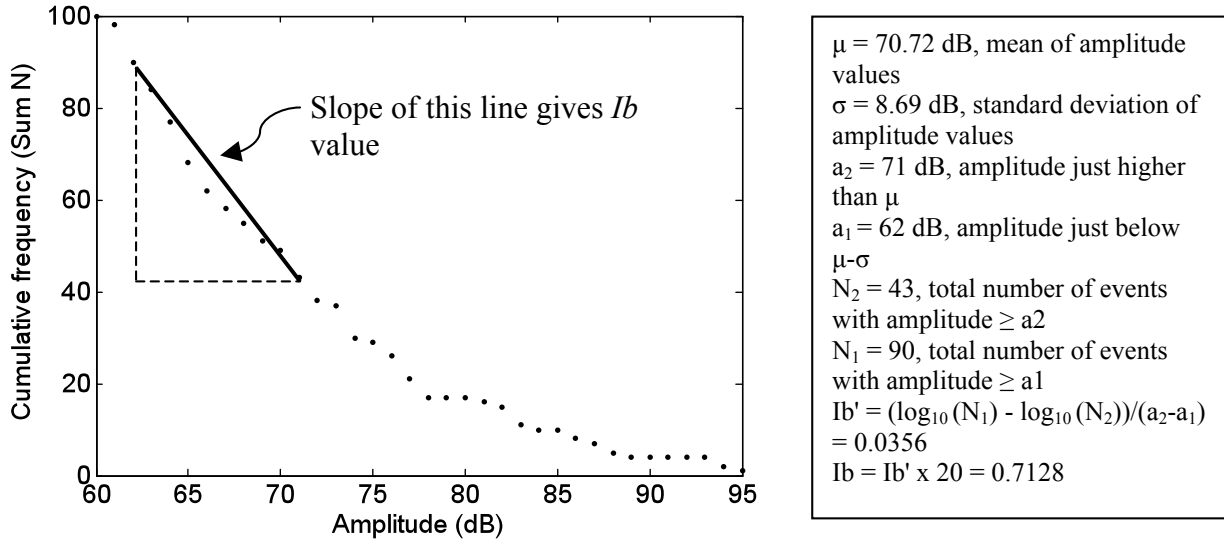


Fig. 8. Ib value calculation for first set of 100 events for 1 mm/min loading.

The plots in Fig. 9 show that the lowest Ib values are around 0.5 and occur at the yielding region (marked by an ellipse). As this region is known to be the areas of significant AE generation [15, 16], the occurrence of lowest Ib value has provided an accurate indication of damage occurrence. Further, higher activity (large number of AE event rates) and higher intensity events (events with higher amplitude) are also seen at the same time. These observations indicate that the instance of damage initiation is predicted by the lowest Ib-value.

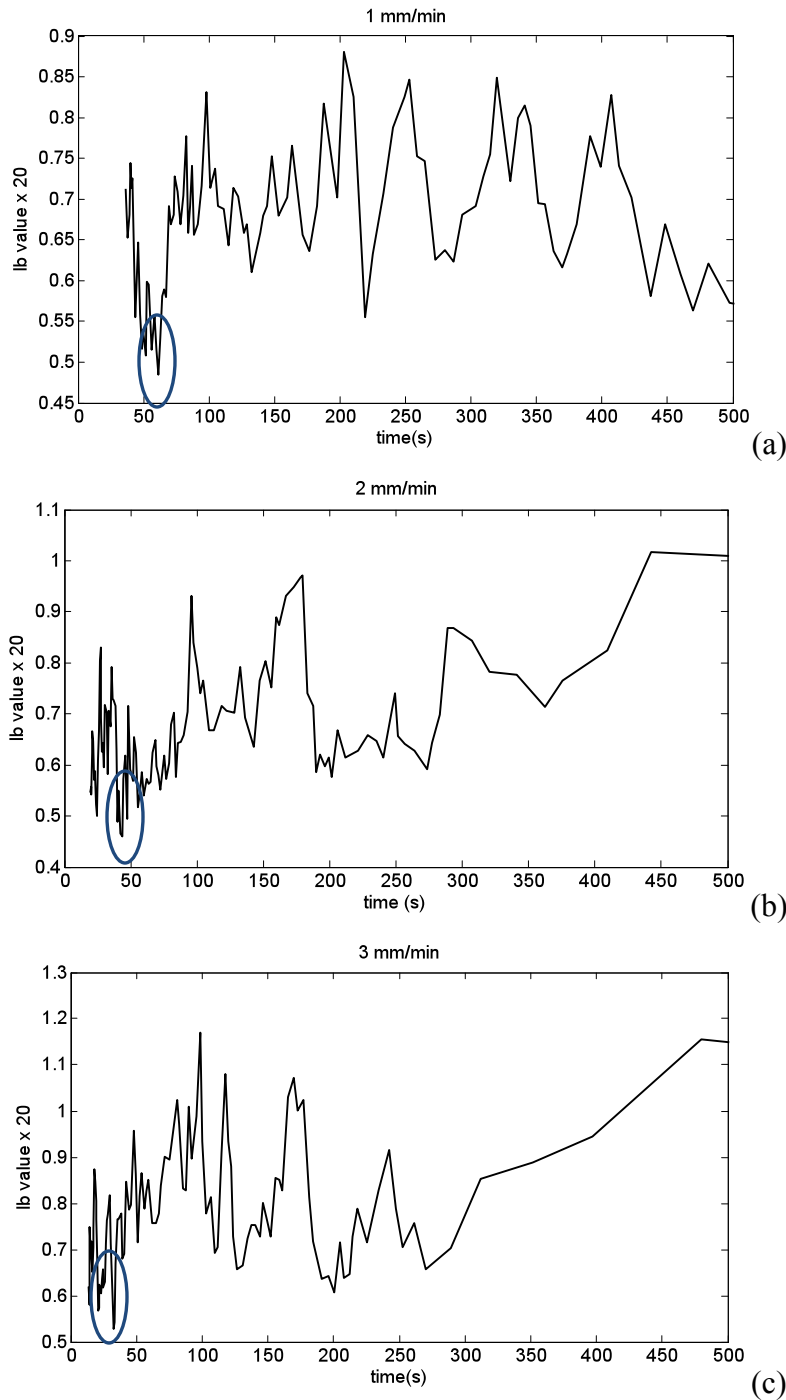


Fig. 9. Ib-values for three loading conditions.

## Conclusions

The main aims of this study were to study some aspects of two important issues in application of AE technique for SHM of engineering structures, namely source differentiation and damage quantification. The results from the tests indicate that energy distribution in different frequency bands can be a suitable tool for differentiating signals from different sources. Further, if a template signal from a known source is available, it can be compared with subsequently obtained experimental signals using maximum cross-correlation value and average magnitude coherence values to judge signal similarity, thus performing source differentiation.

Regarding damage quantification, use of Ib-value to analyse recorded AE data from three-point bending load gave promising results. The studies on the use of Ib-value in brittle materials such as concrete and rock have found the value of around 1 at around the fracture point. The observations in the study show that the onset of plasticity, indicating the instance of damage initiation, was predicted by the lowest Ib-value.

More study on data analysis tools for source differentiation and damage quantification will further increase the effectiveness of AE technique for SHM of engineering structures.

## References

1. Holford, K.M. and R.J. Lark, *Acoustic emission testing of bridges*, in *Inspection and monitoring techniques for bridges and civil structures*, G. Fu, ed. 2005, Woodhead, pp. 183-215.
2. Hamstad, M.A. and J.D. McColskey, *Detectability of slow crack growth in bridge steels by acoustic emission*. Materials Evaluation, 1999. **57**(11): 1165-1174.
3. Grosse, C.U., et al., *Improvements of AE technique using wavelet algorithms, coherence functions and automatic data analysis*. Construction and building Materials, 2004. **18**(3): p. 203-213.
4. Qi, G., *Wavelet-based AE characterization of composite materials*. NDT&E International, 2000. **33**(3): 133-144.
5. Eaton, M., et al., *Use of macro fibre composite transducers as acoustic emission sensors*. Remote Sensing, 2009. **1**(2): 68-79.
6. Kurz, J.H., et al. *Similarity matrices as a new feature for acoustic emission analysis of concrete*. in *26th European Conference on Acoustic Emission Testing*. 2004. Berlin: DGZfP. pp. 769-775.
7. Carpinteri, A., G. Lacidogna, and G. Niccolini, *Critical behaviour in concrete structures and damage localization by acoustic emission*. Key Engineering Materials, 2006. **312**: 305-310.
8. Colombo, S., I.G. Main, and M.C. Forde, *Assessing damage of reinforced concrete beam using 'b-value' analysis of acoustic emission signals*. Journal of materials in civil engineering, 2003. **15**(3): 280-286.
9. Carpinteri, A., G. Lacidogna, and S. Puzzi, *From criticality to final collapse: Evolution of the 'b-value' from 1.5 to 1.0*. Chaos, Solitons and Fractals, 2009. **41**(2): 843-853.
10. Shiotani, T., et al., *Application of AE improved b-value to quantitative evaluation of fracture process in concrete materials*. Journal of acoustic emission, 2001. **19**: 118-133.
11. Rao, M.V.M.S. and K.J.P. Lakshmi, *Analysis of b-value and improved b-value of acoustic emissions accompanying rock fracture*. Current Science, 2005. **89**(9). 1577-1582.
12. Mathworks, *MATLAB Users Guide*. 2009: Natick, MA.
13. Auger, F., et al., *Time-Frequency Toolbox - For use with MATLAB*. 1996, CNRS (France) and Rice University (USA).
14. Kurz, J.H., et al., *Stress drop and stress redistribution in concrete quantified over time by the b-value analysis*. Structural health monitoring, 2006. **5**(1): 69-81.
15. Mukhopadhyay, C.K., et al., *Acoustic emission during tensile deformation of annealed and cold-worked AISI type 304 austenitic stainless steel*. Journal of materials science, 1993. **28**: 145-154.
16. Han, Z., H. Luo, and H. Wang, *Effects of strain rate and notch on acoustic emission during the tensile deformation of a discontinuous yielding material*. Materials Science and Engineering A, 2011. **528**(13-14): 4372-4380.